How to cite: *Angew. Chem. Int. Ed.* **2023,** *62,* e202301193
doi.org/10.1002/anie.202301193

*Immunoassays*

# Quantitative Point of Care Tests for Timely Diagnosis of Early-Onset Preeclampsia with High Sensitivity and Specificity

*Sahar Masoumeh Ghorbanpour[+], Shihui Wen[+], Tu'uhevaha J Kaitu'u-Lino, Natalie J. Hannan, Dayong Jin, and Lana McClements**

**Abstract:** Preeclampsia is a heterogeneous and multi-organ cardiovascular disorder of pregnancy. Here, we report the development of a novel strip-based lateral flow assay (LFA) using lanthanide-doped upconversion nanoparticles conjugated to antibodies targeting two different biomarkers for detection of preeclampsia. We first measured circulating plasma FKBPL and CD44 protein concentrations from individuals with early-onset preeclampsia (EOPE), using ELISA. We confirmed that the CD44/FKBPL ratio is reduced in EOPE with a good diagnostic potential. Using our rapid LFA prototypes, we achieved an improved lower limit of detection: 10 pg ml$^{-1}$ for FKBPL and 15 pg ml$^{-1}$ for CD44, which is more than one order lower than the standard ELISA method. Using clinical samples, a cut-off value of 1.24 for CD44/FKBPL ratio provided positive predictive value of 100 % and the negative predictive value of 91 %. Our LFA shows promise as a rapid and highly sensitive point-of-care test for preeclampsia.

[*] S. Masoumeh Ghorbanpour,[+] Assoc. Prof. L. McClements
School of Life Sciences & Institute for Biomedical Materials and Devices, Faculty of Science, University of Technology Sydney
Sydney, NSW, 2007 (Australia)
E-mail: lana.mcclements@uts.edu.au

Dr. S. Wen,[+] Prof. D. Jin
Institute for Biomedical Materials and Devices, School of Mathematical and Physical Sciences, Faculty of Science, University of Technology Sydney
Sydney, NSW, 2007 (Australia)

Dr. S. Wen,[+] Prof. D. Jin, Assoc. Prof. L. McClements
ARC Research Hub for Integrated Device for End-user Analysis at Low-levels (IDEAL), Faculty of Science, University of Technology Sydney
Sydney, NSW, 2007 (Australia)

Prof. T.'u. J Kaitu'u-Lino, Prof. N. J. Hannan
Department of Obstetrics & Gynaecology, Mercy Hospital for Women, The University of Melbourne
Heidelberg (Australia)
and
Mercy Perinatal, Mercy Hospital for Women
Heidelberg (Australia)

[+] These authors contributed equally to this work.



## Introduction

Preeclampsia is a cardiovascular complication that can be fatal for pregnant individuals and their offspring. It manifests during the second half of pregnancy (after 20 weeks' gestation), and it is the leading cause of morbidity and mortality in pregnancy.[1] If not detected in a timely manner, it can lead to severe pregnancy complications including eclampsia, HELLP (haemolysis, elevated liver enzymes, low platelet count) syndrome, preterm birth and death.[2] The phenotypes of preeclampsia are classified according to the gestational age of diagnosis: (i) early-onset preeclampsia is diagnosed prior to 34 weeks of gestation, (ii) late-onset preeclampsia is diagnosed from 34 weeks of gestation, and (iii) postpartum preeclampsia that can develop up to 4 weeks after delivery.[3] Although late-onset preeclampsia is responsible for the vast majority of preeclampsia cases, early-onset preeclampsia is particularly important as it is more likely to be associated with placental insufficiency and progressive deterioration of maternal condition.[4] Currently, the established criteria for preeclampsia diagnosis include new onset of hypertension after 20 weeks of gestation, combined with the development of new onset of symptoms including proteinuria, liver dysfunction, renal failure, neurological and/or hematological complications, impaired uteroplacental or fetoplacental perfusion.[2b,5] Although preeclampsia-related mortality can be significantly reduced through early detection, close monitoring, and timely treatment of the symptoms, reliable diagnosis of this dangerous condition is still challenging.[6] This is because preeclampsia is a heterogeneous and multifactorial disease with varying symptoms and features among pregnant individuals. Consequently, there is an urgent need to develop sensitive point-of-care tests that can identify the likelihood of evolving preeclampsia and lead to timely diagnosis, enabling immediate clinical decisions.

FKBPL is a divergent member of the immunophilin protein family that plays a critical role in angiogenesis, inflammation and vascular development.[7] FKBPL is mainly secreted by fibroblasts and human microvascular endothelial cells and has an anti-angiogenic function.[8] A cross-sectional study revealed a positive association between plasma FKBPL concentration and B-type Natriuretic Peptide (BNP), an established biomarker for cardiovascular disease, and FKBPL was positively correlated with echocardiographic parameters of diastolic dysfunction.[9] Additionally, FKBPL plasma concentration is negatively correlated with HbA1c and blood glucose in people with type 2 diabetes

 

mellitus (T2D) compared to people without T2D.[9] As such, FKBPL seems to play an important role in the pathogenesis and diagnosis of cardio-metabolic disease. FKBPL is also one of the primary mediators of cellular stress response that signals through the CD44 pathway.[8] Recently, FKBPL and CD44 were identified, for the first time, as promising predictive and diagnostic biomarkers of preeclampsia with an essential role in its pathogenesis.[10] Based on the plasma concentrations measured in pregnant individuals who proceeded to develop preeclampsia or healthy controls, the CD44/FKBPL ratio could be used to predict the risk of preeclampsia at week 20 of gestation hence stratifying those high-risk pregnancies with evolving preeclampsia towards timely diagnosis.[10] Whilst this work was based on the ELISA assay, CD44 and FKBPL utility was not yet explored in the point of care settings.

Simple and low-cost strip-based lateral flow assays (LFAs), such as pregnancy tests, have been widely used for point of care detection of various diseases.[11] They often use colorimetric reagents as signal tags to give an off/on signal that is readable by the naked eye or a smartphone. Compared with lab-based bulky instruments, these transportable and low-cost devices are simple, affordable and portable, and can give a fast response without the need of trained personnel, sophisticated instruments and complex sample preparation.[12] Lanthanide-doped upconversion nanoparticles (UCNPs) can combine two or more lower-energy photons into one higher-energy photon for a range of emerging applications, including single-molecule detection and sensing,[13] *in vivo* bioimaging,[14] colour- and lifetime-based optical multiplexing,[15] and super-resolution imaging.[16] Compared to the colorimetric changes of gold NPs, which suffers from limited sensitivity and quantitative ability, the intensity changes of UCNPs can be utilized to accurately quantify the concentration of detected biomarkers. Recently, we employed highly doped UCNPs with enhanced luminescence intensity, as sensitive nanoprobes for strip-based biomarker detection.[12]

In this study, we established a rapid lateral flow method for the diagnosis of preeclampsia by quantifying the concentration (and determining a ratio) of two biomarkers: FKBPL and CD44, which was compared to the well-established ELISA method. This is the first study that sought to (i) evaluate the plasma concentration of a novel vascular-related protein, FKBPL and its target CD44, in established early-onset preeclampsia and (ii) design and develop first-in-class point of care assay combining the novel UCNPs with FKBPL and CD44 biomarkers. This platform could establish a rapid and reliable method for the diagnosis of preeclampsia, ultimately enabling faster clinical decisions and better outcomes for pregnant individuals and their offspring (Figure 1).

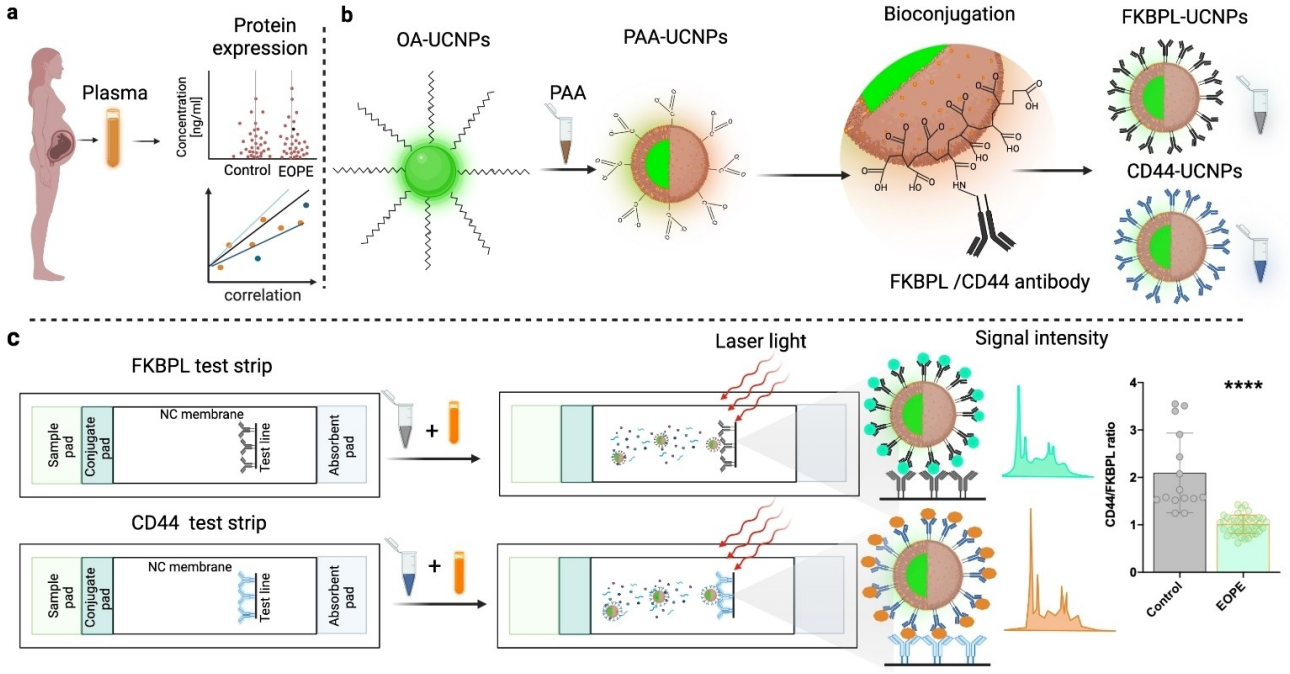


***Figure 1.*** Schematic summary of the study design. a) Healthy and early-onset preeclampsia plasma samples were interrogated for circulating protein concentration of FKBPL and CD44. b) The UCNPs surface was modified with poly-acrylic acid (PAA) and bioconjugated with FKBPL (FKBPL-UCNPs) or CD44 (CD44-UCNPs) antibodies. c) Lateral flow test strips for FKBPL and CD44 detection were designed. The FKBPL and CD44 signal intensity in early-onset preeclampsia and control plasma samples were measured using the corresponding test strips and CD44/FKBPL ratio was calculated.

## Results and Discussion

### FKBPL and CD44 Proteins as Reliable Diagnostic Markers for Early-onset Preeclampsia

Given FKBPL's crucial role in developmental, physiological and pathological angiogenesis and vasculature,[7b] through binding to the cell surface protein, CD44,[17] we determined FKBPL and CD44 plasma concentration in early-onset preeclampsia compared to normotensive pregnant controls by ELISA. There was no significant difference between the early-onset preeclampsia and the control group in terms of maternal age, gestational age (at blood collection) and gravidity. However, BMI was higher, and as expected, gestational age at delivery was significantly lower and, systolic blood pressure (sBP), diastolic (dBP) and mean arterial blood pressure (MABP), were significantly higher, in the early-onset preeclampsia group (Table 1).

In the early-onset preeclampsia group, FKBPL plasma concentration was significantly higher compared to the control group ($p=0.009$, Figure 2a). In contrast to FKBPL, CD44 plasma concentration was significantly lower in early-

***Table 1:*** Clinical characteristics of normotensive pregnancies and pregnancies with established early-onset preeclampsia whose plasma was collected.[a]

| | Control ($n=15$) | Early-onset preeclampsia ($n=45$) | P value |
|---|---|---|---|
| Age (years) | 32.46 ± 5.22 | 30.95 ± 5.09 | 0.36 |
| Gestational age at blood collection (weeks) | 29.08 ± 3.54 | 29.25 ± 2.65 | 0.85 |
| Gestational age at delivery (weeks) | 39.07 ± 1.15 | 29.47 ± 2.75 | **< 0.0001** |
| BMI (kg/m$^2$) | 25.14 ± 5.63 | 30.50 ± 7.74 | **0.02** |
| sBP (mmHg) | 120.4 ± 8.02 | 174.2 ± 15.06 | **0.01** |
| dBP (mmHg) | 75 ± 6.34 | 103.5 ± 10.40 | **0.0003** |
| MABP (mmHg) | 88.98 ± 7.19 | 127.2 ± 10.39 | **0.0004** |
| Gravidity | 2.30 (1–5) | 2 (1–5) | 0.27 |
| Infant birth weight (g) | 3490 ± 341.5 | 1181 ± 509.2 | **< 0.0001** |

[a] All clinical characteristics were presented as mean ± SD. Bold indicated statistical significance ($p<0.05$). Key: BMI, body mass index; sBP, systolic blood pressure; dBP, diastolic blood pressure; MABP, mean arterial blood pressure.

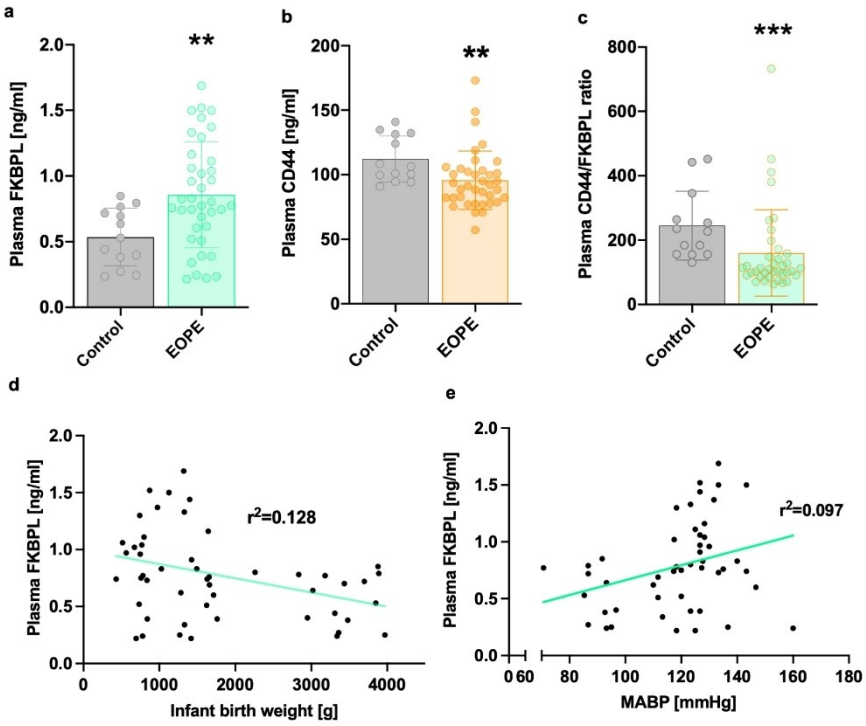


***Figure 2.*** Circulating FKBPL and CD44 concentration in the plasma of individuals with early-onset preeclampsia vs normotensive controls. a) Plasma FKBPL concentration is higher in early-onset preeclampsia ($n=38$) compared with controls ($n=13$); b) CD44 concentration is lower in the plasma of individuals with early-onset preeclampsia ($n=38$) compared with controls ($n=13$); c) CD44/FKBPL ratio is lower in early-onset preeclampsia ($n=38$) compared with controls ($n=13$); d) FKBPL concentration is negatively correlated with infant birth weight ($r^2=0.128$, $p=0.01$); e) There is a significant positive association between FKBPL concentration and MABP ($r^2=0.097$, $p=0.028$). EOPE: early-onset preeclampsia. Each data point represents a single patient. Data plotted as mean ± SD; $n\geq13$; $n=51$ total, *$p<0.05$, **$p<0.01$, ***$p<0.001$, ****$p<0.0001$.

onset preeclampsia compared to controls ($p=0.005$, Figure 2b). The CD44/FKBPL ratio was also significantly lower in early-onset preeclampsia compared to the control group ($p=0.0004$, Figure 2c). Using linear regression analysis, a significant negative association was observed between FKBPL plasma concentration and gestational age at delivery ($r^2=0.150$, $p=0.005$, Figure S1a) or infant birth weight ($r^2=0.128$, $p=0.01$, Figure 2d), whereas a significant positive association was observed between plasma FKBPL concentration and MABP ($r^2=0.097$, $p=0.028$, Figure 2e). There was no association between plasma FKBPL concentration and BMI (Figure S1b). There was no significant association between CD44 and gestational age at delivery, BMI, MABP or infant birth weight (Figures S1c–f). In terms of the CD44/FKBPL ratio, there was no significant correlation with gestational age at delivery, BMI, MABP or infant birth weight (Figures S1g–k).

Since there was a difference in BMI between the early-onset preeclampsia and healthy control groups, and BMI is a known confounding factor for preeclampsia,[18] we performed a partial correlation between the biomarkers and the presence of early-onset preeclampsia adjusted for BMI. The correlation remained significant suggesting BMI does not influence the concentration of FKBPL, CD44 and CD44/FKBPL ratio (FKBPL $r=0.315$, $p=0.027$, CD44 $r=-0.371$, $p=0.009$, CD44/FKBPL $r=-0.311$, $p=0.03$) and this is aligned with a non-significant correlation between the biomarkers and BMI (Figures S1b, d and h). Based on the CD44/FKBPL ROC curve (AUC = 0.81, $p=0.0007$), patients with a cut-off value (CD44/FKBPL ratio) less than 152.1 (sensitivity of 73.68 % and specificity of 92.31 %, Table S1 and Figure S2) are 9.6 times more likely to be diagnosed with early-onset preeclampsia. According to the CD44/FKBPL ratio of less than 152.1, the positive and negative predictive values for detection of early-onset preeclampsia are 90 % and 77 %, respectively.

### *Surface Modification and Characterization of UCNPs*

Highly doped nanoparticles with 40 % $Yb^{3+}$ and 4 % $Er^{3+}$ were synthesized based on the previously reported method (Figure 3a).[19] The growth of inert shells was used to passivate non-radiative pathways to surface quenchers to improve their brightness (Figure 3b).[20] After the shell coating, the size of UCNPs increased from 31 nm to 36 nm, indicating the thickness of the inert shell of 2.5 nm (Figure S3a-b). In order to transfer UCNPs from hydrophobic to

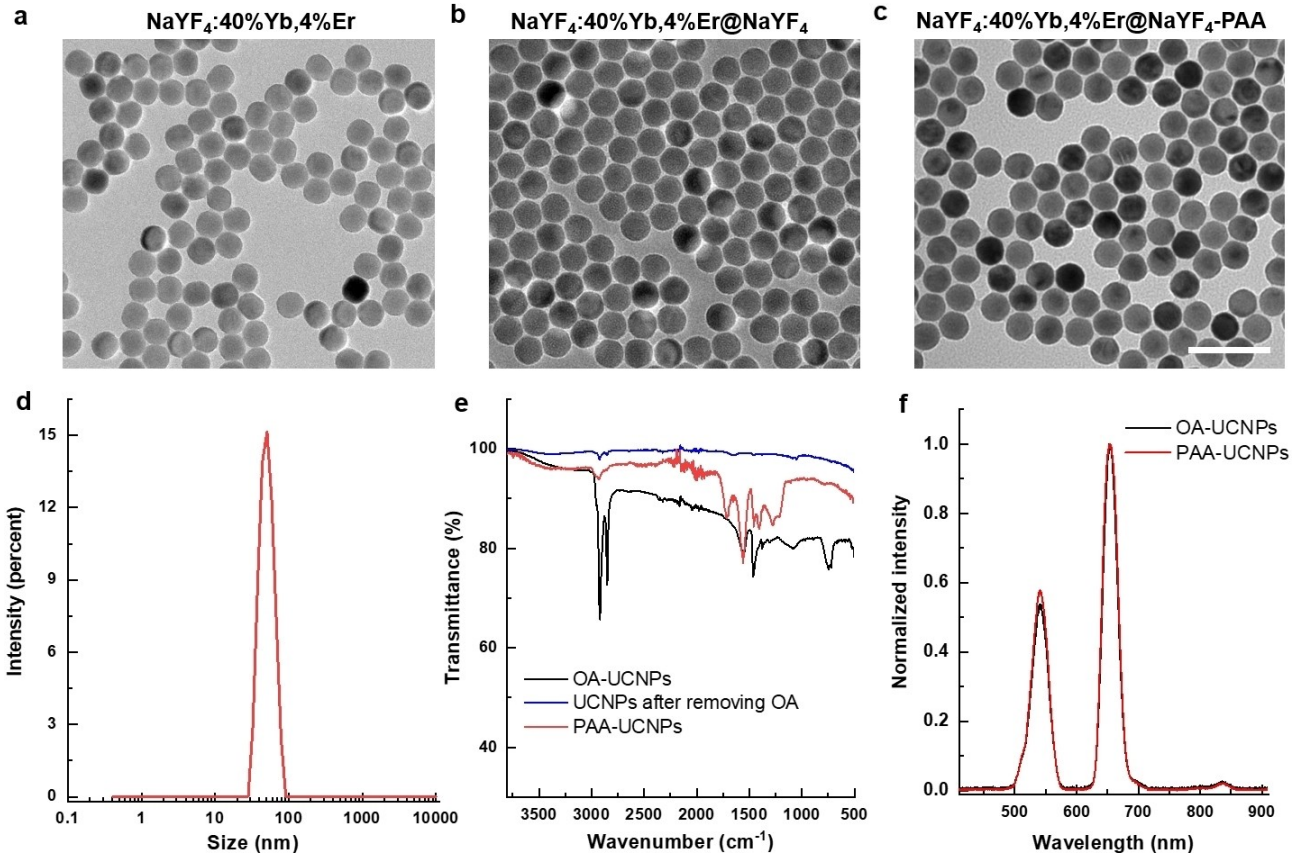


***Figure 3.*** Synthesis and characterization of UCNPs. a) TEM images of $NaYF_4$:40%Yb,4%Er; b) $NaYF_4$:40%Yb,4%Er@$NaYF_4$; c) $NaYF_4$:40%Yb,4%Er@$NaYF_4$ modified with PAA; Scale bar is 100 nm. d) Dynamic Light Scattering (DLS) CONTIN plot of UCNPs modified with PAA; e) Fourier transform infrared spectra (FTIR) of UCNPs with OA and without OA; f) Luminescence spectra of UCNPs under 980 nm excitation before and after the modification of PAA.

hydrophilic state, we modified the UCNPs with poly-acrylic acid (PAA). The TEM results confirmed that the surface modifications did not change the morphology of UCNPs (Figure 3c), and the size of the particles remains uniform with a diameter of around 36 nm after two-step surface modifications (Figure S3c). The DLS data showed the average size of PAA-UCNPs in the solution was around 65 nm with narrow size distribution (Figure 3d). To measure the stability of PAA-UCNPs in water solution, we systematically tested the DLS size of the nanoparticles from 1 day to 7 days after PAA modification. The result showed no change in size for the PAA-UCNPs over one week (Figure S3d).

Fourier transform infrared (FTIR) spectroscopy also confirmed the existence of oleate ligands on the surface of OA-UCNPs, which has typical peaks at 2900 and 1625 $cm^{-1}$ belonging to the $-CH_2-$, $-CH_3$, C=C and C=O vibration stretches of OA ligands, respectively (Figure 3e and Figure S3e). The absence of these characteristic peaks indicates surface OA was mostly removed after acidic treatment. FTIR confirmed the successful coating of PAA ligands on the surface of PAA-UCNPs. The spectrum showed clear absorption bands of PAA at 1638 $cm^{-1}$ (asymmetric stretching vibrations of $CO_2$), and 1563 $cm^{-1}$ (asymmetric stretching vibrations of CO) (Figure 3e), which agrees with the FTIR spectrum of PAA at pH 8.0 (Figure S3e). Since the PAA polymer contained carboxylic groups that can be ionized in water solutions, the surface charge of the nanoparticles was −25 mV as measured by zeta potential measurement. Under the 980 nm excitation, OA-UCNPs and PAA-UCNPs display similar optical properties with multiple emission bands at 540 and 654 nm (Figure 3f), corresponding to the $^4S_{3/2}\rightarrow{}^4I_{15/2}$, $^4F_{9/2}\rightarrow{}^4I_{15/2}$ transitions of $Er^{3+}$, respectively.

When we conjugated antibodies (monoclonal FKBPL and monoclonal CD44, antibody) onto the surface of PAA-UCNPs, AnteoTech Nano Kit was used to enable the reaction between the carboxylic groups of PAA-UCNPs and the amino groups of antibodies. TEM images demonstrated that the conjugation of antibodies did not disrupt the monodispersion of the nanoparticles. The DLS measurements showed that the size of the antibody/PAA-UCNPs in solution increased from 65 nm to 96 nm and 104 nm for anti-FKBPL and anti-CD44 antibodies, respectively (Figure S4). Notably, the zeta potential of the antibody/PAA-UCNPs in solution also increased from −25 mV to −15 mV and −13 mV for anti-FKBPL and anti-CD44, respectively. For the conjugated product FKBPL-UCNPs, the A280 values of the initial concentration of monoclonal FKBPL antibody (0.23) and supernatants (0.04) indicate 82.6 % of antibody was coupled to PAA-UCNPs, with each nanoparticle having around 89 antibody molecules (Figure S5a,d). Similarly, according to the A280 values of the initial concentration of monoclonal CD44 antibody (0.22) and supernatants (0.052) in each nanoparticle contained roughly 41 CD44 antibody molecules (Figure S5b,d). To verify the activity of the monoclonal FKBPL antibody after conjugation onto the surface of PAA-UCNPs, a sandwich ELISA experiments was performed and analyzed with confocal microscopy. The experimental group containing 25 $ng\,mL^{-1}$ FKBPL protein displayed a significant brighter fluorescence signal compared with the control group without any FKBPL protein, which indicates the construction of a sandwich structure between capture antibody, protein, and the detection antibody on the surface of FKBPL-UCNPs ($p=0.0117$, Figures S6a–b). Using the same ELISA experimental set-up, the signal intensity of the experimental group containing 25 $ng\,mL^{-1}$ CD44 protein was significantly higher than the control group ($p=0.0031$, Figures S6c–d).

### *Development of UCNPs-based Lateral Flow Assay*

To show the potential of the FKBPL- and CD44-UCNPs for rapid and accurate quantification of FKBPL and CD44 protein concentration in plasma, we designed the strip-based LFA (Figure 4a). In our design, FKBPL and CD44 proteins with a different concentration in the running buffer were mixed with the bioconjugated UCNPs for 10 min. The sample mix was then added to the sample pad, which migrated along the nitrocellulose membrane until the protein was bound to the capture antibody on the test line. The luminescent intensity of the UCNPs on the test line was read using a strip reader equipped with a 980 nm laser. As shown in Figure 4b, the luminescent intensity of the test line increased with the protein concentration in the running buffer (from 0.025 to 100 $ng\,ml^{-1}$), indicating that the nanoprobes correlate with the concentration of the targets.

Based on the one-phase exponential decay function model, a relationship was obtained between the signal intensity of UCNPs at 654 nm and FKBPL protein with concentrations ranging from 0.025 to 100 $ng\,mL^{-1}$ ($R^2=0.998$, Figure 4b). The limit of detection for FKBPL protein was around 10 $pg\,mL^{-1}$ which was ≈15 times lower than that of the ELISA method.[21] LOD in this work is defined as the target concentration where the intensity is equal to the sum of the background noise and three times the standard deviation above the background noise. Similarly, there was a clear positive correlation between the fluorescence signals of UCNPs and CD44 concentration (range from 0.04 to 100 $ng\,mL^{-1}$) with the limit of detection calculated at around 15 $pg\,mL^{-1}$ ($R^2=0.994$, Figure 4c) which was ≈9 times lower than that obtained by ELISA.[22]

We individually evaluated this LFA′s specificity for both FKBPL and CD44. We tested the detection signal intensity for FKBPL with a concentration of 2.5 $ng\,mL^{-1}$ in the presence and absence of a high concentration of CD44 (400 $ng\,mL^{-1}$) using FKBPL-UCNPs LFA. There was no significant reduction or increase of the signals for FKBPL detection in the presence of CD44 ($p=0.099$; Figure 4d). Similarly, there were no significant changes in the CD44 detection signal in the presence of high concentration of FKBPL (400 $ng\,mL^{-1}$) using CD44-UCNPs LFA ($p=0.618$; Figure 4e). The results indicate that there were negligible cross-interactions between FKBPL and CD44.

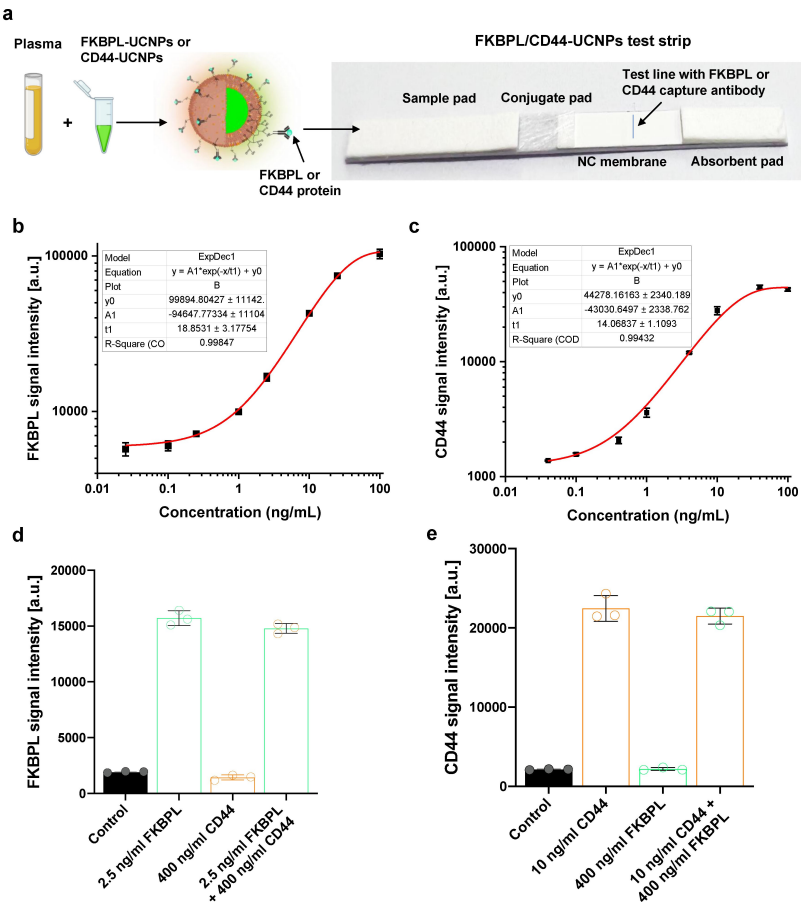


***Figure 4.*** Characterization of FKBPL and CD44 UCNPs-base LFA. a) schematic illustration and image of FKBPL and CD44 strip; b) The calibration curve of the FKBPL-UCNPs LFA for the detection of FKBPL protein at concentrations of 0.025, 0.1, 0.25, 1, 2.5, 10, 25, and 100 ng mL$^{-1}$, $R^2 = 0.998$ ; c) The calibration curve of the CD44-UCNPs LFA for the detection of CD44 protein at concentrations of 0.04, 0.1, 0.4, 1, 4, 10, 40, and 100 ng mL$^{-1}$, $R^2 = 0.994$; d) There is no reduction in FKBPL signal in the presence of high concentrations of CD44 in samples (2.5 ng mL$^{-1}$ FKBPL and 400 ng mL$^{-1}$ CD44); e) There is no reduction in CD44 signal in the presence of high concentrations of FKBPL in samples (10 ng mL$^{-1}$ CD44 and 400 ng mL$^{-1}$ FKBPL).

### *Detection of the CD44/FKBPL Biomarker Ratio in Clinical Samples Using LFA*

Given satisfactory FKBPL and CD44 biomarker detection performance of the developed LFA, the next step was to validate the UCNPs-based LFA for rapid and reliable detection of the concentration of FKBPL and CD44 in clinical samples. This type of test will be beneficial for the diagnosis of preeclampsia at the point of care settings. Based on the limit of detection of our LFA, we reduced the plasma concentration by diluting the samples (1:40) in running buffer and mixing with FKBPL-UCNPs or CD44-UCNPs probes. Then UCNPs-plasma conjugates flew through the strips, and the fluorescence signal from FKBPL and CD44 was measured separately (Figure 1c). While the plasma FKBPL signal was significantly higher (≅20 %) in early-onset preeclampsia compared to the control group ($p < 0.0001$, Figure 5a), there was a significant reduction (≅40 %) in CD44 signal intensity within preeclampsia samples ($p < 0.0001$, Figure 5b). This translated to a much lower CD44/FKBPL intensity ratio in early-onset preeclampsia compared to controls ($p < 0.0001$, Figure 5c), which was aligned with the results of the ELISA test.

Interestingly, AUC increased to 0.98 when FKBPL (AUC = 0.83, $p = 0.0001$, Figure 5d) and CD44 (AUC = 0.93, $p < 0.0001$, Figure 5e) biomarkers were combined as the CD44/FKBPL ratio (AUC = 0.98, $p < 0.0001$, Figure 5f). The ROC curves analysis demonstrated that a cut-off value of 1.24 for the CD44/FKBPL ratio (sensitivity of 90.48 % and specificity of 100 %, Table S2) was appropriate for diagnosing preeclampsia during pregnancy. The positive and negative predictive values based on this cut-off value were respectable 100 % and 91 %, respectively. We further tested the sensitivity of LFAs by mixing the 2.5 ng ml$^{-1}$ of FKBPL or 10 ng ml$^{-1}$ of CD44, spike protein, with plasma samples. Using FKBPL-LFA, we were able to detect the total concentration of FKBPL protein in plasma mixed with 2.5 ng ml$^{-1}$ FKBPL antigen (% Recovery = 97.57 % ± 20.31 %; Figure S7a and Table S3). Similarly, CD44-UCNPs LFA was able to detect the total concentration of CD44 protein in plasma mixed with 10 ng ml$^{-1}$ CD44 protein (% Recovery = 110.2 % ± 12.78 %; Figure S7b and Table S4).

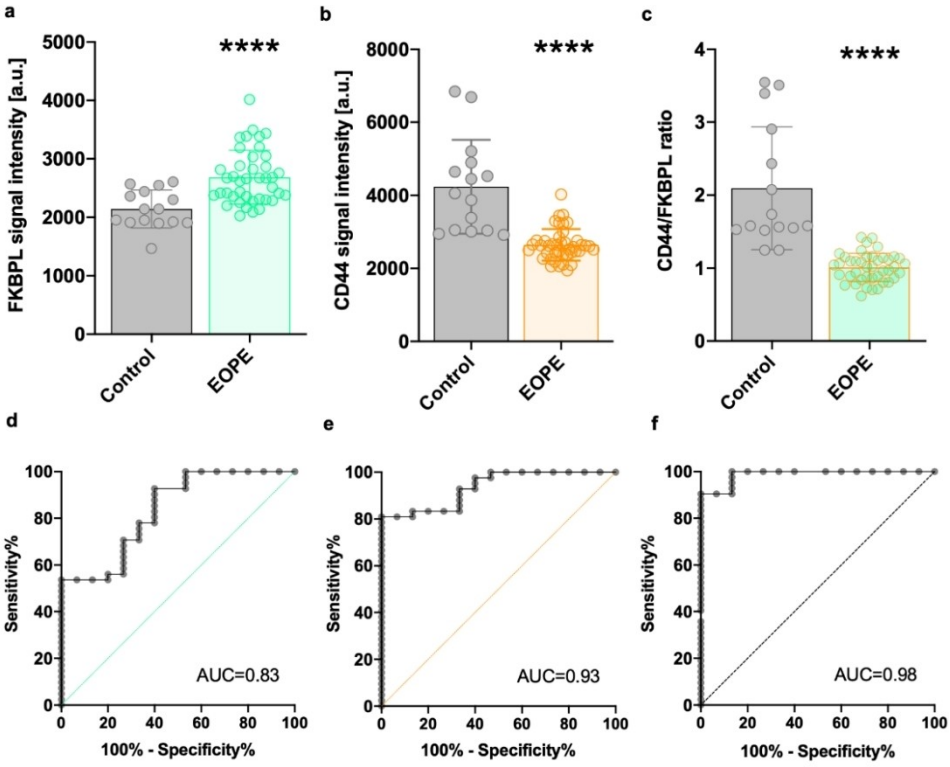


***Figure 5.*** Using UCNPs-based LFAs to determine differences in FKBPL and CD44 intensities between early-onset preeclampsia and healthy pregnancy. a) FKBPL signal intensity is higher in early-onset preeclampsia ($n=42$) compared to the control group ($n=15$); b) CD44 signal intensity is lower in early-onset preeclampsia ($n=42$) compared to controls ($n=15$); c) CD44/FKBPL ratio is around 50% lower in early-onset preeclampsia ($n=42$) compared to the control group ($n=15$); d) ROC curve of FKBPL with AUC 0.83, $p=0.0001$; e) ROC curve of CD44 with AUC of 0.93, $p<0.0001$; (f) ROC curve of CD44/FKBPL ratio with AUC of 0.98, $p<0.0001$. EOPE: early-onset preeclampsia. Each data point represents a single patient. Data plotted as mean ± SD; $n=57$ total, *$p<0.05$, **$p<0.01$, ***$p<0.001$, ****$p<0.0001$.

Preeclampsia is a multisystem and multifactorial cardiovascular disorder that occurs in the final stages of pregnancy or postpartum. Although preeclampsia can contribute to intrauterine growth restriction, maternal and perinatal morbidity, and mortality around the world,[23] the only known cure at present is delivery of the baby and placenta.[24] However, this is often premature and can lead to complications and hospitalization.[25] Due to inter-patient variations in symptoms and features of preeclampsia and different phenotypes of preeclampsia, timely diagnosis is still challenging particularly in rural and remote areas, which is critical for good pregnancy outcomes. In this study, we validated FKBPL and CD44 as useful diagnostic biomarkers for early-onset preeclampsia and developed a first-in-class point of care LFA for detection and quantification of FKBPL and CD44 plasma protein concentration. The results are obtainable within a short period of time (≈15 min), and the FKBPL- and CD44-point of care LFAs were validated using clinical plasma samples showing high sensitivity and specificity.

FKBPL plays a critical role in angiogenesis and has been implicated in the pathogenesis of preeclampsia.[10,26] We have previously demonstrated that FKBPL and its target protein, CD44, can predict the risk of preeclampsia at 20 weeks of gestation and facilitate the diagnosis of preeclampsia, particularly late-onset preeclampsia.[10] Additionally, high FKBPL plasma concentrations are also observed in patients with diastolic dysfunction and cardiovascular disease[9] and FKBPL shows increased expression in 3D cardiac spheroids exposed to plasma from individuals with late-onset preeclampsia compared to healthy controls.[27] Here, plasma FKBPL is also increased and CD44 & CD44/FKBPL ratio decreased in early-onset preeclampsia compared to normotensive pregnancies, which is reflective of restricted angiogenesis and endothelial dysfunction,[8] hallmark features in the development of preeclampsia.[28] Interestingly, we also demonstrated that a higher circulating concentration of FKBPL,[8] is associated with infant growth restriction and shorter gestational age at delivery in pregnancy, which is typical for early-onset preeclampsia.[28b] Studies have shown that individuals with preeclampsia exhibit elevated concentrations of anti-angiogenic factors, including soluble fms-like tyrosine kinase 1 (sFlt1) and soluble endoglin (sEng)[29] that may act in concert with FKBPL restricting the development of the placental vascular network, thereby inhibiting normal placental growth and leading to earlier delivery. However, Yakundi et al. demonstrated that FKBPL-mediated effects are independent of VEGF signalling.[7b] Preeclampsia is also associated with an increase in the production of pro-inflammatory cytokines, including tumour necrosis factor alpha (TNF-α)[30] and interleukin (IL)-6.[8] In contrast, anti-

inflammatory cytokines such as IL-10[31] and IL-4[32] are decreased, often leading to a reduction in VE-cadherin[33] and ultimately impaired vascular integrity.[34] The positive correlation between high circulating FKBPL concentration and high MABP in this cohort may reflect the upregulation of FKBPL as a compensatory mechanism to restore endothelial dysfunction following the reduction of FKBPL early in pregnancy and preceding preeclampsia as reported previously.[10] The FKBPL-based therapeutic peptide, AD-01, has been shown to inhibit endothelial dysfunction and inflammatory cytokines in low FKBPL settings using in vitro and in vivo models suggesting that AD-01 may have therapeutic potential at low doses to restore FKBPL early in pregnancy that may prevent preeclampsia if proven safe in pregnancy.[35]

Here, for the first time, we established a prototype of the nanoparticles-based point of care testing that has the potential for rapid and accurate detection of preeclampsia by quantifying the circulating CD44 to FKBPL protein ratio in plasma samples. The high-quality UCNPs, employed in this work, have presented significant advances in this field of biodetections, due to their high brightness, nonbleaching, nonblinking, and uniformity in size and intensity.[36] In this paper, we incorporated the unique properties of UCNPs and novel biomarkers, FKBPL and its target, CD44, to design high-sensitivity LFA to aid diagnosis of preeclampsia in pregnancy, particularly in the point of care settings. Compared to previous research on UCNPs-based LFA,[12,37] we have demonstrated our capability to quantitatively detect two different biomarkers related to the same disease. By leveraging the ratio changes of the different biomarkers, we have made disease diagnosis more accurate. Using clinical samples, our rapid test showed significantly improved sensitivity (90.5 % vs. 73.7 %) and specificity (100 % vs. 92.3 %) compared to the ELISA method. This could provide a novel method in the future for assessing the risk of preeclampsia at 20 weeks of pregnancy and detecting cases of evolving preeclampsia towards timely diagnosis. While the cost of the strips is ≈$2, the strip reader can be more expensive due to the need for a 980 nm laser and related optical system. However, based on our previous work, we estimate that the total cost of the strip reader should not exceed $100.[12] With the advancement of strip reader technology that can detect signals from different positions, it is possible to include both a test line for FKBPL and a test line for CD44 in a single strip, providing an optimal approach for detecting these simultaneously. Also, high-performance antibodies and simultaneously multiplexed detections will significantly improve the accuracy of preeclampsia diagnosis towards better pregnancy outcomes.

## Conclusion

In summary, in established early-onset preeclampsia, circulating plasma FKBPL and CD44 concentrations were increased and decreased, respectively, with the CD44/FKBPL ratio also decreased. This study showed for the first time that FKBPL and CD44 can be specifically used for early-onset preeclampsia diagnosis where high FKBPL plasma concentration is associated with restricted foetal growth and early delivery. The potential of FKBPL and its target, CD44, as novel biomarkers for early-onset preeclampsia diagnosis could increase the likelihood of more accurate and timely diagnosis of preeclampsia and prevent pregnancy complications. In addition, we developed an innovative and quantitative first-in-class nanoparticles-based LFA for rapid and accurate preeclampsia diagnosis in the point of care settings capable of quantifying the ratio of CD44 and FKBPL. Interestingly, we achieved the ultra-sensitive detection of both CD44 and FKBPL with the limit of detection of 15 and 10 $pg\,mL^{-1}$, respectively, without cross-talk. Finally, we applied our rapid LFA to quantitively detect the concentration of both CD44 and FKBPL in clinical plasma samples, where the biomarker intensity ratio in the preeclampsia group was 50 % lower compared to the controls with excellent sensitivity and specificity, showing improved utility compared to our previous findings.[10,38] This fully developed LFA could be potentially applied in detecting a wide range of biomarkers for early diagnosis of various diseases in the point of care settings, which would be particularly beneficial for remote and rural areas.

## Acknowledgements

In this study, the authors acknowledge the use of Leica Stellaris confocal microscope at the Microbial Imaging Facility (MIF) of the Australian Institute for Microbiology & Infection (AIMI) in the Faculty of Science at the University of Technology Sydney. We would like to thank A/Prof. Louise Cole and Prof. James Brown for providing scientific insight and technical assistance with microscopy and statistical analysis, respectively. For the creation of the graphical abstract and schematics in the Figures, the authors acknowledge the use of BioRender. This research was supported by International Research Scholarship (S.G.), UTS President Scholarship (S.G.), Future Leader Fellowship Level 1 from the National Heart Foundation of Australia (L.M., 106628), Australian Research Council (ARC) Discovery Early Career Researcher Award Scheme (S.W., DE220100846), ARC Laureate Fellowship Program (D.J., FL210100180), Australian Research Council Industrial Research Hub for Integrated Device for End-User Analysis at Low-Levels (IH150100028), Australia China Science and Research Fund Joint Research Centre for Point-of-Care Testing (ACSRF658277, SQ2017YFGH001190), and the Faculty of Science Seed Funding (UTS). Open Access publishing facilitated by University of Technology Sydney, as part of the Wiley - University of Technology Sydney agreement via the Council of Australian University Librarians.

## Conflict of Interest

A/Prof Lana McClements is an inventor on two FKBPL-related patents for preeclampsia and Prof Dayong Jin is an

inventor on a patent related to analyte quantification used in this work.

## Data Availability Statement

The data that support the findings of this study are available from the corresponding author upon reasonable request.

**Keywords:** CD44 · FKBPL · Point of Care Testing · Preeclampsia · Upconversion Nanoparticles


[1] E. A. Steegers, P. Von Dadelszen, J. J. Duvekot, R. Pijnenborg, *Lancet* **2010**, *376*, 631–644.

[2] a) A. C. Staff, S. J. Benton, P. von Dadelszen, J. M. Roberts, R. N. Taylor, R. W. Powers, D. S. Charnock-Jones, C. W. Redman, *Hypertension* **2013**, *61*, 932–942; b) A. Tranquilli, G. Dekker, L. Magee, J. Roberts, B. Sibai, W. Steyn, G. Zeeman, M. Brown, *Pregnancy Hypertens.* **2014**, *4*, 97–104.

[3] a) M. Portelli, B. Baron, *J. Pregnancy* **2018**, *2018*; b) L. A. Matthys, K. H. Coppage, D. S. Lambers, J. R. Barton, B. M. Sibai, *Am. J. Obstet. Gynecol.* **2004**, *190*, 1464–1466.

[4] S. Shahul, H. Ramadan, A. Mueller, J. Nizamuddin, R. Nasim, J. L. Perdigao, S. Chinthala, A. Tung, S. Rana, *Pregnancy Hypertens.* **2017**, *10*, 251–255.

[5] M. A. Brown, L. A. Magee, L. C. Kenny, S. A. Karumanchi, F. P. McCarthy, S. Saito, D. R. Hall, C. E. Warren, G. Adoyi, S. Ishaku, *Hypertension* **2018**, *72*, 24–43.

[6] T. M. MacDonald, S. P. Walker, N. J. Hannan, S. Tong, J. Tu′uhevaha, *EBioMedicine* **2022**, *75*, 103780.

[7] a) H. D. McKeen, K. McAlpine, A. Valentine, D. J. Quinn, K. McClelland, C. Byrne, M. O′Rourke, S. Young, C. J. Scott, H. O. McCarthy, D. G. Hirst, T. Robson, *Endocrinology* **2008**, *149*, 5724–5734; b) A. Yakkundi, R. Bennett, I. Hernández-Negrete, J.-M. Delalande, M. Hanna, O. Lyubomska, K. Arthur, A. Short, H. McKeen, L. Nelson, C. M. McCrudden, R. McNally, L. McClements, H. O. McCarthy, A. J. Burns, R. Bicknell, A. Kissenpfennig, T. Robson, *Arterioscler., Thromb., Vasc. Biol.* **2015**, *35*, 845–854.

[8] A. Valentine, M. O′Rourke, A. Yakkundi, J. Worthington, M. Hookham, R. Bicknell, H. O. McCarthy, K. McClelland, L. McCallum, H. Dyer, H. McKeen, D. Waugh, J. Roberts, J. McGregor, G. Cotton, I. James, T. Harrison, D. G. Hirst, T. Robson, *Clin. Cancer Res.* **2011**, *17*, 1044–1056.

[9] A. S. Januszewski, C. J. Watson, V. O'Neill, K. McDonald, M. Ledwidge, T. Robson, A. J. Jenkins, A. C. Keech, L. McClements, *Sci. Rep.* **2020**, *10*, 21655.

[10] N. Todd, R. McNally, A. Alqudah, D. Jerotic, S. Suvakov, D. Obradovic, D. Hoch, J. R. Hombrebueno, G. L. Campos, C. J. Watson, M. Gojnic-Dugalic, T. P. Simic, A. Krasnodembskaya, G. Desoye, K. A. Eastwood, A. J. Hunter, V. A. Holmes, D. R. McCance, I. S. Young, D. J. Grieve, L. C. Kenny, V. D. Garovic, T. Robson, L. McClements, *J. Clin. Endocrinol. Metab.* **2021**, *106*, 26–41.

[11] V. Shirshahi, G. Liu, *TrAC, Trends Anal. Chem.* **2021**, *136*, 116200.

[12] H. He, B. Liu, S. Wen, J. Liao, G. Lin, J. Zhou, D. Jin, *Anal. Chem.* **2018**, *90*, 12356–12360.

[13] a) J. Zhao, D. Jin, E. P. Schartner, Y. Lu, Y. Liu, A. V. Zvyagin, L. Zhang, J. M. Dawes, P. Xi, J. A. Piper, E. M. Goldys, T. M. Monro, *Nat. Nanotechnol.* **2013**, *8*, 729–734; b) F. Wang, S. Wen, H. He, B. Wang, Z. Zhou, O. Shimoni, D. Jin, *Light: Sci. Appl.* **2018**, *7*, 18007.

[14] G. Bao, S. Wen, G. Lin, J. Yuan, J. Lin, K.-L. Wong, J.-C. G. Bünzli, D. Jin, *Coord. Chem. Rev.* **2021**, *429*, 213642.

[15] a) X. Zhu, X. Liu, H. Zhang, M. Zhao, P. Pei, Y. Chen, Y. Yang, L. Lu, P. Yu, C. Sun, J. Ming, I. M. Ábrahám, A. Mohamed El-Toni, A. Khan, F. Zhang, *Angew. Chem.* **2021**, *133*, 23737–23743; b) Y. Fan, P. Wang, Y. Lu, R. Wang, L. Zhou, X. Zheng, X. Li, J. A. Piper, F. Zhang, *Nat. Nanotechnol.* **2018**, *13*, 941–946; c) J. Liao, J. Zhou, Y. Song, B. Liu, Y. Chen, F. Wang, C. Chen, J. Lin, X. Chen, J. Lu, D. Jin, *Nano Lett.* **2021**, *21*, 7659–7668.

[16] a) C. Lee, E. Z. Xu, Y. Liu, A. Teitelboim, K. Yao, A. Fernandez-Bravo, A. M. Kotulska, S. H. Nam, Y. D. Suh, A. Bednarkiewicz, B. E. Cohen, E. M. Chan, P. J. Schuck, *Nature* **2021**, *589*, 230–235; b) Y. Liang, Z. Zhu, S. Qiao, X. Guo, R. Pu, H. Tang, H. Liu, H. Dong, T. Peng, L.-D. Sun, J. Widengren, Q. Zhan, *Nat. Nanotechnol.* **2022**, *17*, 524–530; c) C. Chen, F. Wang, S. Wen, Q. P. Su, M. C. Wu, Y. Liu, B. Wang, D. Li, X. Shan, M. Kianinia, I. Aharonovich, M. Toth, S. P. Jackson, P. Xi, D. Jin, *Nat. Commun.* **2018**, *9*, 3290; d) Y. Liu, Y. Lu, X. Yang, X. Zheng, S. Wen, F. Wang, X. Vidal, J. Zhao, D. Liu, Z. Zhou, C. Ma, J. Zhou, J. A. Piper, P. Xi, D. Jin, *Nature* **2017**, *543*, 229–233.

[17] A. Yakkundi, L. McCallum, A. O'Kane, H. Dyer, J. Worthington, H. D. McKeen, L. McClements, C. Elliott, H. O. McCarthy, D. G. Hirst, T. Robson, *PloS one* **2013**, *8*, e55075.

[18] a) D. Mrema, R. T. Lie, T. Østbye, M. J. Mahande, A. K. Daltveit, *BMC pregnancy and childbirth* **2018**, *18*, 56; b) P.-Y. Robillard, G. Dekker, M. Scioscia, F. Bonsante, S. Iacobelli, M. Boukerrou, T. C. Hulsey, *PloS one* **2019**, *14*, e0223888.

[19] a) D. Liu, X. Xu, Y. Du, X. Qin, Y. Zhang, C. Ma, S. Wen, W. Ren, E. M. Goldys, J. A. Piper, S. Dou, X. Liu, D. Jin, *Nat. Commun.* **2016**, *7*, 10254; b) X. Shan, F. Wang, D. Wang, S. Wen, C. Chen, X. Di, P. Nie, J. Liao, Y. Liu, L. Ding, P. J. Reece, D. Jin, *Nat. Nanotechnol.* **2021**, *16*, 531–537.

[20] S. Wen, D. Li, Y. Liu, C. Chen, F. Wang, J. Zhou, G. Bao, L. Zhang, D. Jin, *J. Phys. Chem. Lett.* **2022**, *13*, 5316–5323.

[21] "ELISA Kit for FK506 Binding Protein Like Protein (FKBPL) | SEL523Hu | Homo sapiens (Human) CLOUD-CLONE CORP.(CCC), *can be found under* http://www.cloud-clone.com/products/SEL523Hu.html.

[22] "Human CD44 ELISA Kit (ab45912) | Abcam, *can be found under* https://www.abcam.com/human-cd44-elisa-kit-ab45912.html.

[23] a) L. Duley, in *Seminars in perinatology, Vol. 33*, Elsevier, **2009**, pp. 130–137; b) J. P. Souza, *Br. J. Obstet. Gynaecol.* **2014**, *121*, v–viii.

[24] J. Uzan, M. Carbonnel, O. Piconne, R. Asmar, J.-M. Ayoubi, *Vasc. Health Risk Manage.* **2011**, 467–474.

[25] Z. Armaly, J. E. Jadaon, A. Jabbour, Z. A. Abassi, *Front. Physiol.* **2018**, *9*, 973.

[26] S. Annett, G. Moore, A. Short, A. Marshall, C. McCrudden, A. Yakkundi, S. Das, W. G. McCluggage, L. Nelson, I. Harley, N. Moustafa, C. J. Kennedy, A. deFazio, A. Brand, R. Sharma, D. Brennan, S. O′Toole, J. O′Leary, M. Bates, C. O′Riain, D. O′Connor, F. Furlong, H. McCarthy, A. Kissenpfennig, L. McClements, T. Robson, *Br. J. Cancer* **2020**, *122*, 361–371.

[27] C. Richards, K. Sesperez, M. Chhor, S. Ghorbanpour, C. Rennie, C. L. C. Ming, C. Evenhuis, V. Nikolic, N. K. Orlic, Z. Mikovic, M. Stefanovic, Z. Cakic, K. McGrath, C. Gentile, K. Bubb, L. McClements, *Biol. Sex Differ.* **2021**, *12*, 1–14.

[28] a) T. Chaiworapongsa, P. Chaemsaithong, L. Yeo, R. Romero, *Nat. Rev. Nephrol.* **2014**, *10*, 466–480; b) J. Young, *Proc. R. Soc. Med.* **1914**, *7*, 307.

[29] S. E. Maynard, J.-Y. Min, J. Merchan, K.-H. Lim, J. Li, S. Mondal, T. A. Libermann, J. P. Morgan, F. W. Sellke, I. E. Stillman, F. H. Epstein, V. P. Sukhatme, S. Ananth Karumanchi, *J. Clin. Invest.* **2003**, *111*, 649–658.

[30] S. D. Keiser, E. W. Veillon, M. R. Parrish, W. Bennett, K. Cockrell, L. Fournier, J. P. Granger, J. N. Martin, B. Lamarca, *Am. J. Hypertens.* **2009**, *22*, 1120–1125.
[31] A. Hennessy, H. Pilmore, L. Simmons, D. Painter, *J. Immunol.* **1999**, *163*, 3491–3495.
[32] L. Arriaga-Pizano, L. Jimenez-Zamudio, F. Vadillo-Ortega, A. Martinez-Flores, T. Herrerias-Canedo, C. Hernandez-Guerrero, *J. Soc. Gynecol. Invest.* **2005**, *12*, 335–342.
[33] S. Flemming, N. Burkard, M. Renschler, F. Vielmuth, M. Meir, M. A. Schick, C. Wunder, C.-T. Germer, V. Spindler, J. Waschke, N. Schlegel, *Cardiovasc. Res.* **2015**, *107*, 32–44.
[34] D. A. Sawant, B. Tharakan, A. Adekanbi, F. A. Hunter, W. R. Smythe, E. W. Childs, *Microcirculation* **2011**, *18*, 46–55.
[35] S. L. Annett, S. Spence, C. Garciarena, C. Campbell, M. Dennehy, C. Drakeford, J. Lai, J. K. Dowling, G. Moore, A. Yakkundi, A. Short, D. Sharpe, F. Furlong, J. O'Donnell, G. Cavalleri, S. Kerrigan, I. Tikhonova, P. Johnson, A. Kissenpfennig, T. Robson, bioRxiv 2021.02.24.431422; https://doi.org/10.1101/2021.02.24.431422.
[36] a) X. Di, D. Wang, Q. P. Su, Y. Liu, J. Liao, M. Maddahfar, J. Zhou, D. Jin, *Proc. Natl. Acad. Sci. U. S. A.* **2022**, *119*, e2207402119; b) S. Wen, J. Zhou, K. Zheng, A. Bednarkiewicz, X. Liu, D. Jin, *Nat. Commun.* **2018**, *9*, 2415.
[37] a) T. Ji, X. Xu, X. Wang, Q. Zhou, W. Ding, B. Chen, X. Guo, Y. Hao, G. Chen, *Sens. Actuators, B* **2019**, *282*, 309–316; b) M. Ali, M. Sajid, M. A. U. Khalid, S. W. Kim, J. H. Lim, D. Huh, K. H. Choi, *Spectrochim. Acta, Part A* **2020**, *226*, 117610; c) E. Juntunen, T. Salminen, S. M. Talha, I. Martiskainen, T. Soukka, K. Pettersson, M. Waris, *J. Med. Virol.* **2017**, *89*, 598–605.
[38] S. M. Ghorbanpour, C. Richards, D. Pienaar, K. Sesperez, H. Aboulkheyr Es, V. N. Nikolic, N. Karadzov Orlic, Z. Mikovic, M. Stefanovic, Z. Cakic, A. Alqudah, L. Cole, C. Gorrie, K. McGrath, M. M. Kavurma, M. Ebrahimi Warkiani, L. McClements, *Cell. Mol. Life Sci.* **2023**, *80*, 44.

Manuscript received: January 24, 2023
Accepted manuscript online: April 13, 2023
Version of record online: May 15, 2023